# Discovery, Synthesis, and Evaluation of Small-Molecule Signal Transducer and Activator of Transcription 3 Inhibitors

Zhi-Bing Shi,[a] Dan Zhao,[a] Yan-Yan Huang,[b] Yun Du,[a] Xiang-Rong Cao,[c] Zhu-Nan Gong,[c] Rui Zhao,[b] and Jian-Xin Li*[,a]

[a] *State Key Laboratory of Analytical Chemistry for Life Science, School of Chemistry and Chemical Engineering, Nanjing University; Nanjing 210093, P.R. China:* [b] *Beijing National Laboratory for Molecular Sciences, Laboratory of Analytical Chemistry for Life Science, Institute of Chemistry, Chinese Academy of Sciences; Beijing 100080, P.R. China: and* [c] *Jiangsu Key Laboratory for Molecular and Medical Biotechnology, Nanjing Normal University; Nanjing 210097, P.R. China.* Received August 22, 2012; accepted September 15, 2012

**The signal transducer and activator of transcription 3 (STAT3) oncogene is a promising molecular target and its inhibitors have great potential as anticancer drugs. To identify novel and STAT3-selective inhibitors, a virtual screening based on Specs and Maybridge databases was conducted and a 6,6′-bibenzoxazole type small molecule, compound 3a with a inhibition constant $K_i$ value of 494.32 nM to STAT3 was explored. Further, a novel series of derivatives originally derived from 3a was synthesized and evaluated through cell-based assays using human breast cancer cell lines, MDA-MB-468 and MCF-7 with or without constitutive expression of STAT3, respectively. In the series, 3a, 3c, 3d and 4e showed a better inhibitory activity with a good selectivity. Among them, 3a and 3c significantly inhibited STAT3 protein level and also displayed binding affinity for STAT3 that detected with flow injection analysis-quartz crystal microbalance (FIA-QCM) analysis system. The results provided a new lead for future design and development of potent STAT3 inhibitors.**

**Key words** signal transducer and activator of transcription 3; inhibitor; cancer; bibenzoxazole

The signal transducers and activators of transcription (STATs) are a class of transcription factor proteins with seven members including 1, 2, 3, 4, 5a, 5b and 6 that regulate cell growth and survival by modulating the expression of specific target genes.[1,2] STAT3, a member of STATs family, was identified by homology screening of cDNA libraries.[3] It is found to be activated by epidermal growth factor (EGF), interleukin-6 (IL-6), and several other growth factors and cytokines that share the gpl30 receptor subunit and its homologs.[4] In normal cells, the activation of STAT3 is rapid and transient. Constitutive activation of STAT3 is frequently detected in the specimens from cancer patients with advanced diseases and a number of tumor cell lines, but not in normal epithelial cells, and also identified as an essential step during the transition of normal cells to neoplastic cells.[5,6] The structure of STAT3 is composed of an amino-terminal domain, a coiled-coil domain, a DNA-binding domain, a linker, a Src Homology 2 (SH2) domain, and a transcriptional activation domain.[7] The STAT3 signal pathway is composed of several distinct steps,[8] among them, the dimerization of two STAT3 monomers through SH2 domains is a decisive event for its activation and transcriptional activity.[2] Blocking dimerization through small modules provides a promising approach to the development of molecularly targeted therapies for the treatment of cancers. Since the X-ray structure of STAT3 dimer complexing with DNA was reported by Becker,[9] the design of SH2 inhibitors has been actively performed for anticancer drug discovery.

Currently, two main approaches are being performed in the design of small molecule inhibitors that suppress STAT3 dimerization. The first one is peptidomimetics, such as ISS610,[10] ISS840 and others.[7,11,12] The peptide-based ligands usually achieve quite high binding affinities to STAT3, but they usually have poor or no cellular activity that limits the application prospect of such compounds. The second one is non-peptidic small molecules, most of them, such as S3I-M2001,[13] STA-21,[14] S3I-201,[15] more recent STX-0119,[16] and others[17] were identified through structure-based virtual screening of chemical libraries (Fig. 1). Those compounds are generally cell permeable and have great potential for further research and development, however, most of them have weak binding affinities or a lower selectivity to STAT3. Therefore, there is still a great need to develop novel molecules with better bioactivity and selectivity to STAT3.

In the present study, as an effort to develop novel small molecule STAT3 inhibitors, we report the discovery of a small molecule STAT3 inhibitor, 2,2′-bis(arylsulphonylamino)-6,6′-bibenzoxazoles (**3a**) through a virtual screening of 2 databases, and synthesis of the derivatives originally derived from **3a**. The bioactivity and the selectivity of the compounds were evaluated using two human breast cancer cell lines, MDA-MB-468 and MCF-7 with or without constitutive expression of STAT3, respectively. Furthermore, inhibitory activity of the compounds with potent bioactivity on STAT3 protein level and the binding affinity to STAT3 were also assayed.

## Results and Discussion

As mentioned above, to be activated, STAT3 must firstly form a dimer *via* its SH2 domain and then translocate to the nucleus to targeted genes.[9] Therefore, blocking of the dimerization of STAT3 monomers is directly associated STAT3 inhibitors. In order to discover basic skeleton of the inhibitors, we conducted a virtual screening against the STAT3 SH2 domain using the available databases including Specs with 321374 compounds and Maybridge with 79299 ones. The 3D structures of those compounds were download from ZINC database[18] and used during the docking studies. The crystal structure of dimerized STAT3 at 2.25 Å was obtained from RCSB protein databank (PDB code: 1BG1). Autodock 4.2[19]

The authors declare no conflict of interest.

* To whom correspondence should be addressed. e-mail: lijxnju@nju.edu.cn

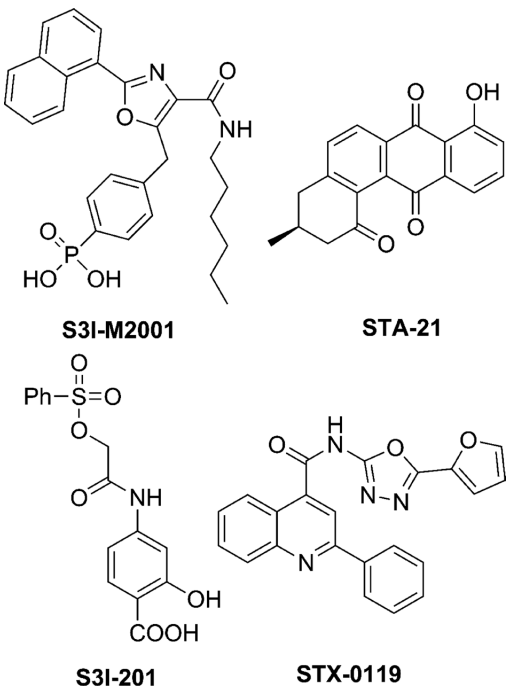


Fig. 1. Typical Small-Molecule STAT3 Inhibitors

and PyRx 0.5 programs were employed to the virtual screening. The AutoDockTools was used to prepare the screening target, chain B of protein 1BG1 and water were removed from the structure and only monomer A was used as the docking target. All hydrogens were added then non polar hydrogens were merged. The Grid center was set SH2 domain and the GridBox was set big enough to cover the entire dimerization interface. Lamarckian Genetic Algorithm was used as a searching method, the number of GA runs was set at 10.

The docking result was rearranged by the binding energy (see Supplementary data), compound **3a** with bis-oxazole skeleton and the binding energy of −8.6 kcal/mol and inhibition constant $K_i$ value of 494.32 nM was selected from the above rows for further study. The predicted binding model (Fig. 2) showed that **3a** has significant interactions with Lys591, Arg636, Lys626, and Gln635. Structure of two analogues **3d** and **3i** were also found in ZINC database (Chart 1), the docking model showed similar interactions with STAT3 SH2 domain.

Bis-oxazole, as an important structure motif exist in many natural products, its derivatives such as hennoxazole and diazonamide A possess significant bioactivities including antifungal, cytotoxic, anthelmintic properties and so on.[20,21]

To confirm the docking results and further get preliminary structure–activity relationship (SAR), compound **3a** and its derivatives **3b**–**l** were designed and synthesized, and the preparations of derivatives **4a**–**g** (monomers) of the half structure of the **3a** were also performed, respectively. The synthetic routes of **3a**–**l**[22] and **4a**–**g** analogues were outlined in Chart 1. Firstly, the commercially available starting materials, arylsulfonamine **1a**–**l** were reacted with carbon disulfide ($CS_2$) in an alkaline medium using *N*,*N*-dimethylformamide (DMF) as solvent to form corresponding intermediates. The intermediates were successively reacted with dimethylsulfate ($Me_2SO_4$) as a methylation agent for 2 h, and the reaction products were treated with water without any isolation processes to provide compounds **2a**–**l**. Then, the heterocyclizations were conducted by reaction of **2a**–**l** with 3,3′-dihydroxybenzidine in the presence of potassium hydroxide (KOH), the products were treated with water and recrystallized in methanol to afford the target compounds **3a**–**l** with satisfactory yields (see Supplementary data).

There were about three methods to synthesize the skeleton of compounds **4a**–**g**.[23—25] Based on the synthetic method of **3a**–**l**, we designed a novel and simple synthetic route of **4a**–**g**. Compounds **2a**–**l** were reacted with *O*-aminophenol with different substitutions, respectively, to directly provide analogues **4a**–**g** with good yields.

With the above synthesized compounds in hand, the antiproliferative activity of the compounds against breast cancer cell line (MDA-MB-468) with constitutive expression of STAT3 was firstly evaluated using a 3-(4,5-dimethylthiazol-2-yl)-2,5-diphenyltetrazolium bromide (MTT) assay. The cells were treated with each compound at the concentrations of 1 $\mu$M, 10 $\mu$M and 100 $\mu$M for 48 h, and the results are summarized in Table 1.

As can been seen from Table 1, the same as the virtual screening result, parent compound **3a** showed a inhibitory activity on MDA-MB-468 cells at 100 $\mu$M concentration, while no activity at 10 $\mu$M. The derivatives **3c**, **3d** and **4e** displayed a better activity compared with **3a** even at 10 $\mu$M. Unfortunately, compounds **3b**, **3e**–**l** and the monomers **4a**–**g** except for **4e** exhibited almost no activity on the cells at 10 $\mu$M. Above data clearly revealed that the substitution at moiety of arylsulfonamide in **3a**–**l** gave a great impact on the activity. *Meta* and *para*-methyl substitutions elevated the activity, while *ortho*-methyl group damaged the activity. The halogen substitutions at any positions of arylsulfonamide moiety deactivated the derivatives. The activity of the monomers (**4a**–**g**) was weaker than that of **3a**–**l**, suggesting that to get better activity, linkage of two basic skeletons was essential, which was almost in agreement with docking results. Compared with reported nonpeptidic small-molecule STAT3 inhibitors such as S3I-M2001 and STX-0119, the present compounds showed comparative activity on MDA-MB-468, while, the compounds were easier to synthesize from sulfonamides compared with preparations of S3I-M2001 and STX-0119 or other small-molecule STAT3 inhibitors.[13–17]

In order to understand the inhibitory selectivity of those compounds with better activity, another breast cancer cell line, MCF-7 cells with no constitutive expression of STAT3 was involved. Four compounds **3a**, **3c**, **3d** and **4e** at 100 $\mu$M concentration were tested. As shown in Fig. 3, four compounds displayed no or very weak suppressive activity toward MCF-7, suggesting those compounds had a good inhibitory selectivity on STAT3.

In order to verify whether the observed inhibitory activity on MDA-MB-468 cells is related to the STAT3 protein, the STAT3 protein level of the cells cultured with compounds **3a**, **3c**, **3d** and **4e** was assayed with a STAT3 ELISA kit. As shown in Fig. 4, **3a** and **3c** at 100 $\mu$M inhibited more than 70% STAT3 protein, while **3d** and **4e** did not display suppressive activity. Because activation of STAT3 leads to cell-cycle progression, anti-apoptotic effects, and tumor invasion and metastasis,[26] the current results revealed that **3a** and **3c** inhibited the proliferation of MDA-MB-468 cells at least *via* a suppression of STAT3 protein content.

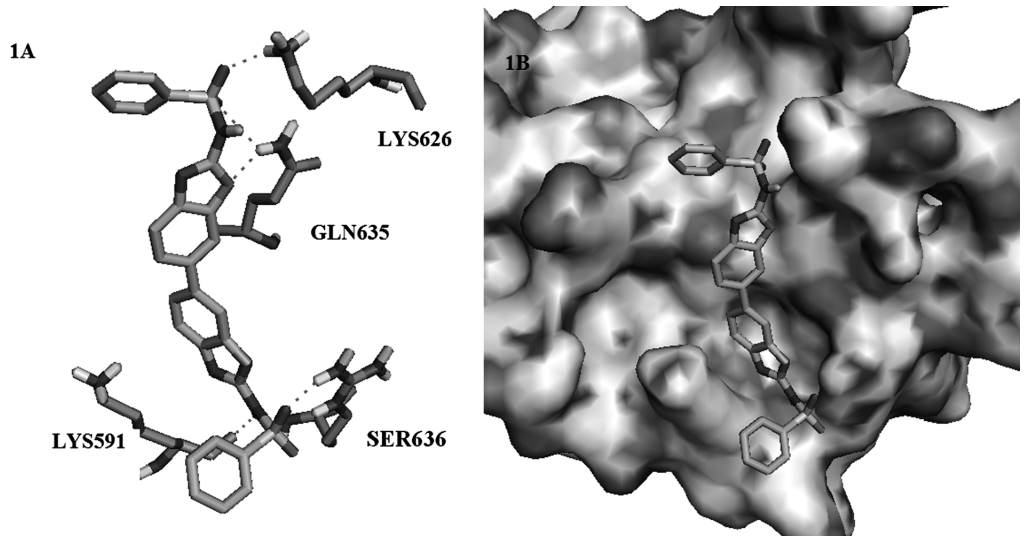


Fig. 2. The Predicted Binding Model of Compound **3a** with the STAT3-SH2 Domain Generated by AutoDock (v4.2)
(A) Only the residues that form hydrogen bonds with **3a** are shown. (B) STAT3-SH2 domain is shown in surface model.

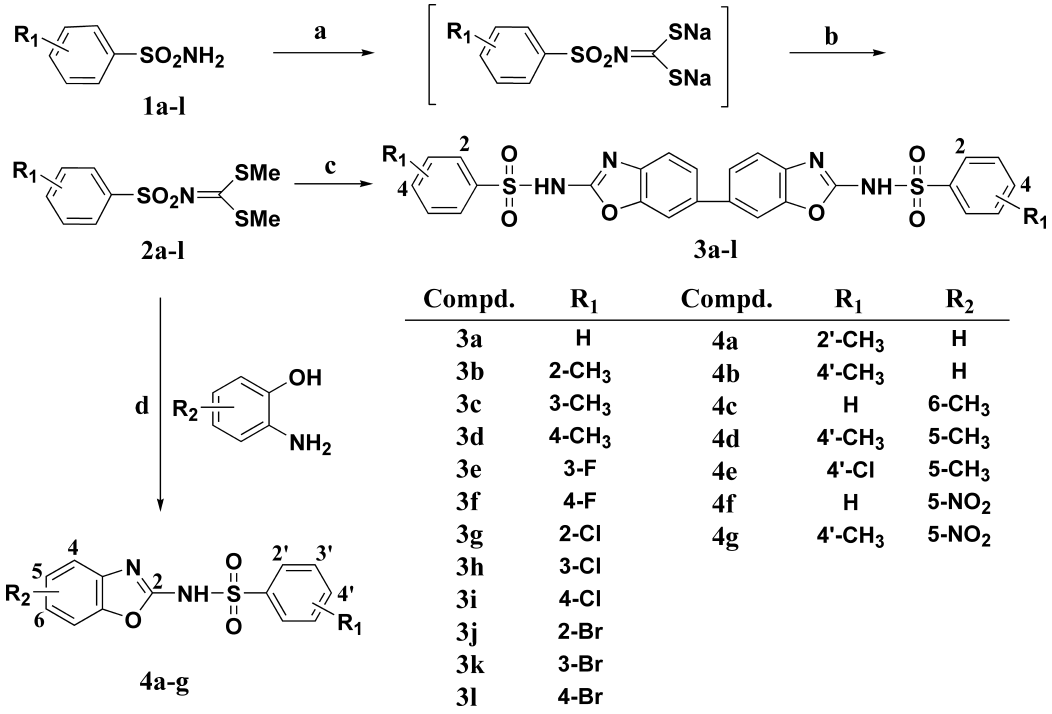


| Compd. | $R_1$ | Compd. | $R_1$ | $R_2$ |
|---|---|---|---|---|
| 3a | H | 4a | 2'-$CH_3$ | H |
| 3b | 2-$CH_3$ | 4b | 4'-$CH_3$ | H |
| 3c | 3-$CH_3$ | 4c | H | 6-$CH_3$ |
| 3d | 4-$CH_3$ | 4d | 4'-$CH_3$ | 5-$CH_3$ |
| 3e | 3-F | 4e | 4'-Cl | 5-$CH_3$ |
| 3f | 4-F | 4f | H | 5-$NO_2$ |
| 3g | 2-Cl | 4g | 4'-$CH_3$ | 5-$NO_2$ |
| 3h | 3-Cl | | | |
| 3i | 4-Cl | | | |
| 3j | 2-Br | | | |
| 3k | 3-Br | | | |
| 3l | 4-Br | | | |

Reagents and conditions: (a) $CS_2$, NaOH, DMF, 0°C; (b) $Me_2SO_4$, RT; (c) 3,3′-Dihydroxybenzidine, KOH, DMF, $N_2$, reflux. (d) KOH, DMF, $N_2$, reflux.
Chart 1. Synthesis of compounds **3a**–**l** and **4a**–**g**

In order to understand the interaction of the inhibitors and STAT3, flow injection analysis-quartz crystal microbalance (FIA-QCM) binding experiments with lead inhibitors **3a** and **3c** were conducted with STAT3 protein immobilized QCM chip. As an extremely sensitive surface mass sensor, quartz crystal microbalance (QCM) has been used for the measurement of mass change in a variety biological studies and has become an ideal method to entirely monitor the association and disassociation processes of molecules in real time without the use of labels.[27] Combined with flow injection analysis (FIA), QCM allows online monitoring of the analyte binding, and provides a much more convenient tool for the determination of real-time study of analytes interactions.[28] Because the commercial available STAT3 solution contains glutathione, to eliminate its interference, a STAT3 modified QCM chip (QCM-S) and only glutathione modified chip (QCM-G) were prepared. The binding curves of frequency *versus* time of **3a** under the optimal conditions were recorded as graphs and illustrated in Fig. 5. From the binding curves, the binding equilibrium constants of **3a** were evaluated to be $4.31\times10^3$ L/mol and $8.50\times10^2$ L/mol on QCM-S (Fig. 5A) and QCM-G (Fig. 5B) chips, respectively. The results clearly demonstrated that **3a** strongly bound with immobilized STAT3. While, **3c** displayed only a weak binding affinity with STAT3, because the binding equilibrium constants were $6.89\times10^2$ L/mol on QCM-S chip and $6.81\times10^2$ L/mol on QCM-G chip, which

Table 1. Inhibitory Effects of Synthesized Compounds on MDB-MA-468 Cells

| Compd. | Inhibition rate (%) | | |
|---|---|---|---|
| | 1 $\mu$M | 10 $\mu$M | 100 $\mu$M |
| **3a** | −8.42±1.53 | 4.73±0.95 | 26.94±1.04* |
| **3b** | −10.50±0.84 | −3.19±1.83 | −6.24±0.10 |
| **3c** | 3.96±1.05 | 16.63±0.81** | 45.41±0.76** |
| **3d** | 5.41±0.47 | 23.60±0.20** | 37.41±0.64** |
| **3e** | −18.61±3.23 | 0.19±1.10 | −5.76±0.57 |
| **3f** | −9.25±0.76 | 4.44±1.15 | 20.59±0.20** |
| **3g** | −15.38±0.53 | −3.19±1.14 | −15.29±0.21 |
| **3h** | −10.81±0.67 | 1.88±0.17 | 8.30±1.70 |
| **3i** | −15.70±0.17 | 2.61±0.99 | 19.65±0.31* |
| **3j** | −16.74±0.25 | 1.83±0.44 | −16.12±1.44 |
| **3k** | −14.14±0.69 | 3.28±0.50 | 20.00±0.55** |
| **3l** | −10.08±0.70 | −0.19±0.17 | 0.24±1.21 |
| **4a** | −9.77±0.50 | −2.99±0.15 | 9.76±0.81 |
| **4b** | −7.17±0.40 | −2.70±0.81 | 17.88±0.93* |
| **4c** | −9.98±0.57 | −0.48±0.69 | 7.76±0.29* |
| **4d** | −6.86±0.40 | 0.87±0.32 | 25.18±0.10* |
| **4e** | −2.60±0.53 | 7.63±0.52* | 22.82±0.49** |
| **4f** | −12.37±0.93 | 1.64±0.67 | −0.94±0.78 |
| **4g** | −10.19±0.46 | 0.29±0.96 | −1.29±0.50 |
| Control | | 0.00±4.01 | |

Human breast cancer cell line MDA-MB-468 with constitutive activation of STAT3 was used for the assay. The inhibition rate cells of control group without any treatment was pegged as 0.00%, while other data were calculated relative to it. Data are expressed as mean±S.D., $n$=4. Significant differences compared with control group, *$p$<0.05, **$p$<0.01. "−" a minus sign of the data means enhancement effect on cell viability.

suggested that the main binding effect was caused from glutathione. As **3c** exhibited inhibitory effect on STAT3 level, it is possible that **3c** might inhibit both STAT3 and upstream kinase, to clarify it, further research work is essential.

## Conclusion

In summary, we have identified a series of novel STAT3 targeting small molecule inhibitors through virtual screening, preliminary structure optimization and *in vitro* assays. Among the compounds, **3a** and **3c** exhibited a potent anti-proliferation activity on STAT3-depend human breast cancer cells with a good selectivity, significantly inhibited STAT3 protein level of MDA-MB-468 cells, and **3a** displayed a strong binding activity on STAT3. The current results provided a new lead for further design and optimization of more potent and selective STAT3 inhibitors as a new class of anticancer drugs.

## Experimental

**General** $^{1}$H- and $^{13}$C-NMR spectra were measured on a Bruker Advance II 300 spectrometer using tetramethylsilane as internal standard. Chemical shift ($\delta$) are reported in parts per million (ppm) and coupling constants $J$ are reported in hertz (Hz), $^{13}$C-NMR spectra were fully decoupled, and the following abbreviations are used: singlet (s), doublet (d), and multiplet (m).

MDA-MB-468 and MCF-7 cells were obtained from the Shanghai Cell Bank of the Chinese Academy of Sciences (Shanghai, China). STAT3 was purchased from PeproTech Inc., U.S.A. Human signal transducer and activator of transcription 3 (STAT3) Kit was from Rapidbio, RB.

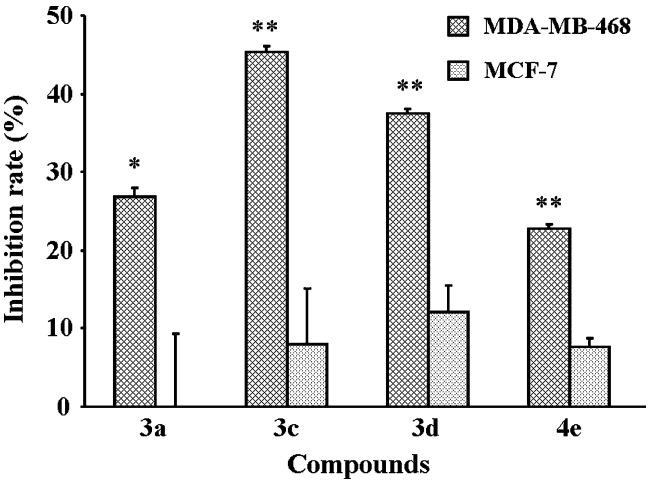


Fig. 3. Inhibitory Effects of the Selective Compounds on MDA-MB-468 and MCF-7

Human breast cancer cells MDA-MB-468 and MCF-7 were treated with 100 $\mu$M selected compounds for 48 h and assayed for viability using MTT method. Control group without any treatment was pegged as 0.00%, while other data were calculated relative to it. Each value represents the mean±S.D., $n$=3. Significant differences compared with control group. *$p$<0.05, **$p$<0.01.

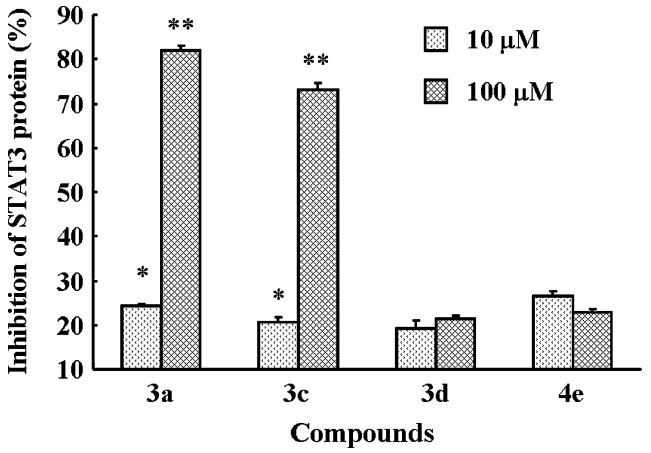


Fig. 4. Effects of the Selective Compounds on STAT3 Protein Content in MDA-MB-468 Cells

Human breast cancer cells MDA-MB-468 were treated with 10 $\mu$M and 100 $\mu$M of selected compounds and the content of STAT3 was assayed with STAT3 ELISA kit. Each value represents the mean±S.D., $n$=3. Significant differences compared with control group (0.00%, the STAT3 concentration was 587.36 pg/mL), *$p$<0.05, **$p$<0.01.

**Chemical Synthesis. General Procedure of Synthesis of *N*-Bis(methylthio)methylene Arylsulfonamide Type Compounds (2a–l)** To a solution of arylsulfonamide (1 mmol) in dried DMF (2 mL) was added NaOH (80 mg) and carbon disulfide (1 mmol) at 0°C over a few minutes. The reaction solution was stirred for 30 min at 0°C, and $Me_2SO_4$ (2 mmol) was added dropwisely over several minutes. After warming up to room temperature, ample water was added and the resulting crystalline precipitate was collected *via* filtration. The filter cake was washed with water, methanol and dried to afford the title compounds.

**General Procedure of Synthesis of 2,2′-Bis(arylsulfonamino)-6,6′-bibenzoxazole (3a–l)** To a solution of 3,3′-dihydroxybenzidine (1 mmol) in dried DMF (8 mL) was added 5 M NaOH solution (0.2 mL), and

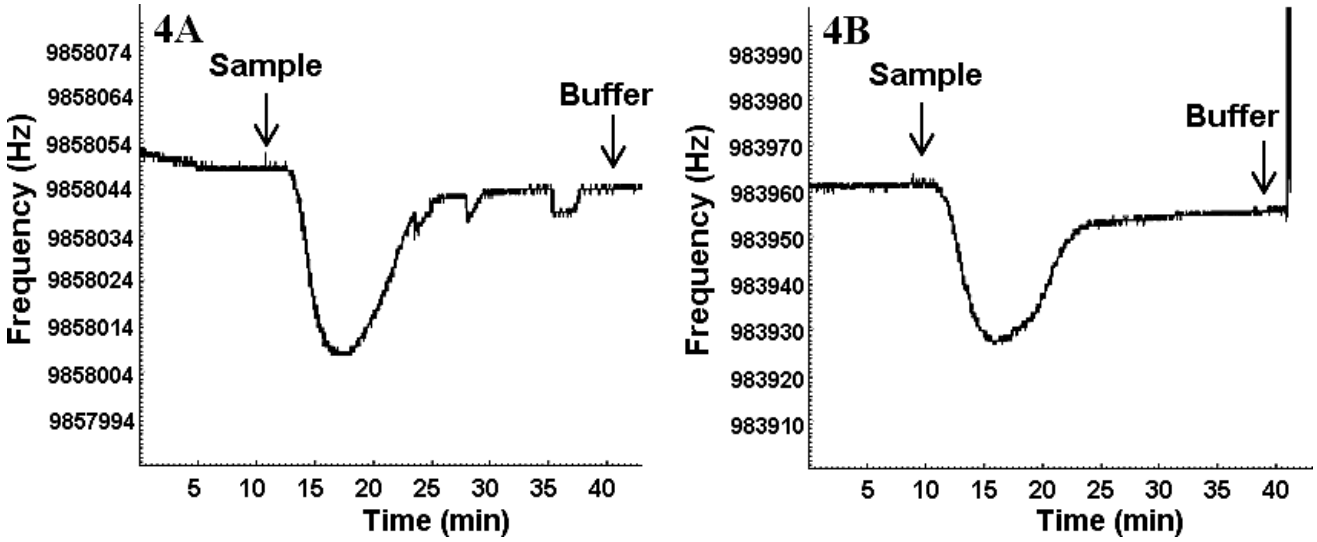


Fig. 5. The Binding Processes of **3a** on STAT3 (A, QCM-S) and Glutathione (B, QCM-G) Immobilized Chips

stirred at room temperature for 30 min. Then, solution of *N*-bis(methylthio)methylene arylsulfonamide (**2**, 2 mmol) in 2 mL DMF was added in dropwise, refluxed under $N_2$ for 8h. After cooling, acetic acid (2 mL) was added. The percipitate obtained after ample water was added, and then washed with water, and recrystallized using methanol to afford the target compounds.

Compound **3a** (436 mg, 80%): $^1$H-NMR (300 MHz, DMSO-$d_6$) $\delta$: 7.94 (m, 4H), 7.87 (s, 1H), 7.60 (m, 8H), 7.37 (d, $J$=7.0 Hz, 2H); $^{13}$C-NMR (75 MHz, DMSO-$d_6$) $\delta$: 156.52, 145.34, 142.63, 135.53, 132.79, 129.75, 129.45, 126.41, 124.37, 112.48, 109.10; positive electrospray ionization (ESI)-MS $m/z$ 547 $[M+1]^+$; high resolution (HR)-MS (ESI): Calcd for $C_{26}H_{19}N_4O_6S_2$ $[M+H]^+$ 547.0746, Found 546.0742.

Compound **3b** (430 mg, 75%): $^1$H-NMR (300 MHz, DMSO-$d_6$) $\delta$: 8.13–7.97 (m, 2H), 7.84 (d, $J$=1.2 Hz, 2H), 7.64–7.45 (m, 4H), 7.36 (m, $J$=10.0, 6.0 Hz, 6H), 2.61 (s, 6H); $^{13}$C-NMR (75 MHz, DMSO-$d_6$) $\delta$: 156.45, 145.29, 140.77, 136.95, 135.52, 132.76, 132.61, 129.81, 127.65, 126.38, 124.36, 112.45, 109.06, 20.20; positive ESI-MS $m/z$ 575 $[M+1]^+$; HR-MS (ESI): Calcd for $C_{28}H_{23}N_4O_6S_2$ $[M+H]^+$ 575.1059, Found 575.1033.

Compound **3c** (459 mg, 80%): $^1$H-NMR (300 MHz, DMSO-$d_6$) $\delta$: 7.84–7.88 (m, 2H), 7.68–7.80 (m, $J$=8.7 Hz, 4H), 7.56–7.64 (m, $J$=7.9 Hz, 2H), 7.51–7.30 (m, 6H), 2.38 (s, 6H). $^{13}$C-NMR (75 MHz, DMSO-$d_6$) $\delta$: 156.52, 145.34, 142.57, 138.33, 135.54, 133.39, 129.82, 129.30, 126.69, 124.58, 123.55, 112.49, 109.10, 21.18; positive ESI-MS $m/z$ 575 $[M+1]^+$; HR-MS (ESI): Calcd for $C_{28}H_{23}N_4O_6S_2$ $[M+H]^+$ 575.1059, Found 575.1042.

Compound **3d** (402 mg, 70%): $^1$H-NMR (300 MHz, DMSO-$d_6$) $\delta$: 7.93–7.74 (m, 6H), 7.61 (d, $J$=8.4 Hz, 2H), 7.36 (d, m, 6H), 2.35 (s, 6H); $^{13}$C-NMR (75 MHz, DMSO-$d_6$) $\delta$: 156.59, 145.41, 143.00, 139.92, 135.50, 129.96, 129.84, 126.50, 124.33, 112.50, 109.05, 21.32; positive ESI-MS $m/z$ 575 $[M+1]^+$; HR-MS (ESI): Calcd for $C_{28}H_{23}N_4O_6S_2$ $[M+H]^+$ 575.1059, Found 575.1051.

Compound **3e** (436 mg, 75%): $^1$H-NMR (300 MHz, DMSO-$d_6$) $\delta$: 7.88 (d, $J$=1.1 Hz, 2H), 7.82–7.69 (m, 4H), 7.56–7.67 (m, 4H), 7.54–7.42 (m, 2H), 7.38 (d, $J$=8.3 Hz, 2H). $^{13}$C-NMR (75 MHz, DMSO-$d_6$) $\delta$: 161.99 (d, $J$=248.1 Hz), 156.85 (s), 145.54 (s), 144.79 (d, $J$=6.6 Hz), 135.57 (s), 131.84 (d, $J$=7.8 Hz), 130.02 (s), 124.39 (s), 122.75 (s), 119.83 (d, $J$=21.1 Hz), 113.60 (d, $J$=24.3 Hz), 112.61 (s), 109.11 (s); positive ESI-MS $m/z$ 583 $[M+1]^+$; HR-MS (ESI): Calcd for $C_{26}H_{17}F_2N_4O_6S_2$ $[M+H]^+$ 583.0558, Found 583.0535.

Compound **3f** (436 mg, 75%): $^1$H-NMR (300 MHz, DMSO-$d_6$) $\delta$: 12.49 (s, 2H), 8.07–7.94 (m, 3H), 7.91–7.79 (m, 3H), 7.61 (d, $J$=8.4 Hz, 2H), 7.47–7.30 (m, 6H); $^{13}$C-NMR (75 MHz, DMSO-$d_6$) $\delta$: 164.44 (d, $J$=243.9 Hz), 156.58 (s), 145.44 (s), 139.10 (s), 135.55 (s), 129.83 (s), 129.50 (d, $J$=9.5 Hz), 126.94 (s), 125.58 (s), 124.39 (s), 116.54 (d, $J$=22.5 Hz), 112.52 (s), 109.11 (s); positive ESI-MS $m/z$ 583 $[M+1]^+$; HR-MS (ESI): Calcd for $C_{26}H_{17}F_2N_4O_6S_2$ $[M+H]^+$ 583.0558, Found 583.0541.

Compound **3g** (442 mg, 72%): $^1$H-NMR (300 MHz, DMSO-$d_6$) $\delta$: 8.14 (m, 2H), 7.97–7.76 (m, 2H), 7.71–7.49 (m, 8H), 7.42 (d, $J$=7.3 Hz, 2H); $^{13}$C-NMR (75 MHz, DMSO-$d_6$) $\delta$: 156.95, 145.24, 139.85, 135.75, 134.65, 134.25, 132.08, 131.31, 129.85, 127.94, 124.54, 112.71, 109.21; positive ESI-MS $m/z$ 615 $[M+1]^+$; HR-MS (ESI): Calcd for $C_{26}H_{17}Cl_2N_4O_6S_2$ $[M+H]^+$ 614.9967, Found 614.9959.

Compound **3h** (461 mg, 75%): $^1$H-NMR (300 MHz, DMSO-$d_6$) $\delta$: 11.72 (s, 2H), 8.00–7.80 (m, 6H), 7.70 (d, $J$= 8.8 Hz, 2H), 7.60 (m, 4H), 7.38 (d, $J$=7.3 Hz, 2H); $^{13}$C-NMR (75 MHz, DMSO-$d_6$) $\delta$ 156.74, 145.47, 144.52, 135.62, 133.97, 132.72, 131.57, 129.78, 126.15, 125.20, 124.45, 112.59, 109.16; positive ESI-MS $m/z$ 615 $[M+1]^+$; HR-MS (ESI): Calcd for $C_{26}H_{17}Cl_2N_4O_6S_2$ $[M+H]^+$ 614.9967, Found 614.9944.

Compound **3i** (462 mg, 75%): $^1$H-NMR (300 MHz, DMSO-$d_6$) $\delta$: 7.94 (m, 4H), 7.88 (d, $J$=1.1 Hz, 2H), 7.62 (m, 6H), 7.37 (d, $J$=8.3 Hz, 2H); $^{13}$C-NMR (75 MHz, DMSO-$d_6$) $\delta$: 156.80, 145.51, 144.68, 135.59, 131.78, 129.93, 128.92, 125.55, 124.42, 122.26, 112.62, 109.13; positive ESI-MS $m/z$ 616 $[M+1]^+$; HR-MS (ESI): Calcd for $C_{26}H_{17}Cl_2N_4O_6S_2$ $[M+H]^+$ 614.9967, Found 614.9961.

Compound **3j** (528 mg, 75%): $^1$H-NMR (300 MHz, DMSO-$d_6$) $\delta$: 8.17 (dd, $J$=7.7, 1.6 Hz, 2H), 7.92–7.78 (m, 4H), 7.70–7.48 (m, 6H), 7.41 (d, $J$=8.3 Hz, 2H); $^{13}$C-NMR (75 MHz, DMSO-$d_6$) $\delta$: 157.01, 152.87, 145.28, 141.58, 135.69, 135.53, 134.19, 130.01, 128.42 (s), 124.51, 120.00, 112.70, 109.20; positive ESI-MS $m/z$ 704 $[M+1]^+$; HR-MS (ESI): Calcd for

$C_{26}H_{17}Br_2N_4O_6S_2$ $[M+H]^+$ 704.8936, Found 704.8920.

Compound **3k** (528 mg, 75%): $^1$H-NMR (300 MHz, DMSO-$d_6$) $\delta$: 8.07 (m, 2H), 7.94 (d, $J$=7.8 Hz, 2H), 7.88 (d, $J$=1.2 Hz, 2H), 7.83 (dd, $J$=8.0, 0.9 Hz, 2H), 7.62 (dd, $J$=8.3, 1.4 Hz, 2H), 7.53 (t, $J$=7.9 Hz, 2H), 7.38 (d, $J$=8.3 Hz, 2H); $^{13}$C-NMR (75 MHz, DMSO-$d_6$) $\delta$: 156.80, 145.51, 144.68, 135.59, 131.78, 130.92, 129.93, 128.92, 125.55, 124.42, 122.26, 112.62, 109.13; positive ESI-MS $m/z$ 704 $[M+1]^+$; HR-MS (ESI): Calcd for $C_{26}H_{17}Br_2N_4O_6S_2$ $[M+H]^+$ 704.8936, Found 704.8931.

Compound **3l** (492 mg, 70%): $^1$H-NMR (300 MHz, DMSO-$d_6$) $\delta$: 7.92–7.83 (m, 6H), 7.77 (d, $J$=8.6 Hz, 4H), 7.61 (d, $J$=8.4 Hz, 2H), 7.37 (d, $J$=8.2 Hz, 2H); $^{13}$C-NMR (75 MHz, DMSO-$d_6$) $\delta$: 156.57, 145.47, 141.95, 135.59, 132.50, 129.71, 128.58, 126.94, 126.50, 125.59, 124.45, 112.53, 109.16; positive ESI-MS $m/z$ 704 $[M+1]^+$; HR-MS (ESI): Calcd for $C_{26}H_{17}Br_2N_4O_6S_2$ $[M+H]^+$ 704.8936, Found 704.8908.

**General Procedure of Synthesis of 4a–g** The synthetic route was similar to that procedure for compound **3a**, but *O*-aminophenols with different substitutions were used instead of 3,3′-dihydroxybenzidine and the equivalent of *O*-aminophenols was equal to compound **2a**.

Compound **4a** (244 mg, 85%): $^1$H-NMR (300 MHz, DMSO-$d_6$) $\delta$: 12.69 (s, 1H), 8.01 (m, 1H), 7.52–7.15 (m, 7H), 2.61 (s, 3H); $^{13}$C-NMR (75 MHz, DMSO-$d_6$) $\delta$: 156.17, 144.42, 140.78, 136.95, 132.73, 132.59, 130.03, 127.65, 126.35, 125.63, 123.93, 112.25, 110.71, 20.19; positive ESI-MS $m/z$ 289 $[M+1]^+$; HR-MS (ESI): Calcd for $C_{14}H_{13}N_2O_3S$ $[M+H]^+$ 289.0647, Found 289.0633.

Compound **4b** (230 mg, 80%): $^1$H-NMR (300 MHz, DMSO-$d_6$) $\delta$: 12.70 (s, 1H), 7.81 (d, $J$=7.8 Hz, 2H), 7.49 (d, $J$=7.8 Hz, 1H), 7.40–7.16 (m, 5H), 2.35 (s, 3H); $^{13}$C-NMR (75 MHz, DMSO-$d_6$) $\delta$: 156.22, 144.45, 143.00, 139.87, 130.07, 129.82, 126.47, 125.62, 123.92, 112.26, 110.72, 21.30; positive ESI-MS $m/z$ 289 $[M+1]^+$; HR-MS (ESI): Calcd for $C_{14}H_{13}N_2O_3S$ $[M+H]^+$ 289.0647, Found 289.0619.

Compound **4c** (231 mg, 80%): $^1$H-NMR (300 MHz, DMSO-$d_6$) $\delta$: 12.65 (s, 1H), 7.98–7.86 (m, 2H), 7.67–7.48 (m, 3H), 7.32 (s, 1H), 7.20 (d, $J$=8.0 Hz, 1H), 7.09 (d, $J$=8.0 Hz, 1H), 2.33 (s, 3H); $^{13}$C-NMR (75 MHz, DMSO-$d_6$) $\delta$: 156.28, 144.62, 142.73, 133.87, 132.71, 129.58, 127.63, 126.38, 126.13, 111.81, 110.99, 21.24; positive ESI-MS $m/z$ 289 $[M+1]^+$; HR-MS (ESI): Calcd for $C_{14}H_{13}N_2O_3S$ $[M+H]^+$ 289.0647, Found 289.0624.

Compound **4d** (241 mg, 82%): $^1$H-NMR (300 MHz, DMSO-$d_6$) $\delta$: 12.61 (s, 1H), 7.80 (d, $J$=8.2 Hz, 2H), 7.35 (d, $J$=8.2 Hz, 3H), 7.12 (s, 1H), 7.01 (d, $J$=8.3 Hz, 1H), 2.34 (s, 3H), 2.33 (s, 3H); $^{13}$C-NMR (75 MHz, DMSO-$d_6$) $\delta$: 156.43, 142.76, 141.63, 137.49, 135.39, 129.97, 129.51, 128.44, 124.50, 112.39, 110.32 (s), 21.28; positive ESI-MS $m/z$ 303 $[M+1]^+$; HR-MS (ESI): Calcd for $C_{15}H_{15}N_2O_3S$ $[M+H]^+$ 303.0803, Found 303.0801.

Compound **4e** (257 mg, 80%): $^1$H-NMR (300 MHz, DMSO-$d_6$) $\delta$: 12.78 (s, 1H), 7.98–7.87 (m, 2H), 7.62 (d, $J$=8.6 Hz, 2H), 7.37 (d, $J$=8.3 Hz, 1H), 7.13 (s, 1H), 7.02 (d, $J$=8.4 Hz, 1H), 2.34 (s, 3H); $^{13}$C-NMR (75 MHz, DMSO-$d_6$) $\delta$: 156.34, 142.94, 142.62, 139.94, 135.27, 130.06, 129.80, 126.45, 124.38, 112.33, 110.25; positive ESI-MS $m/z$ 323 $[M+1]^+$; HR-MS (ESI): Calcd for $C_{14}H_{12}ClN_2O_3S$ $[M+H]^+$ 323.0257, Found 323.0229.

Compound **4f** (264 mg, 83%): $^1$H-NMR (300 MHz, DMSO-$d_6$) $\delta$: 8.13 (dd, $J$=8.9, 2.4 Hz, 1H), 8.03 (d, $J$=2.3 Hz, 1H), 7.99–7.88 (m, 2H), 7.72 (d, $J$=8.9 Hz, 1H), 7.60 (ddd, $J$=16.0, 7.7, 2.1 Hz, 3H); $^{13}$C-NMR (75 MHz, DMSO-$d_6$) $\delta$: 157.23, 148.61, 145.01, 142.20, 133.03, 131.84, 129.50, 126.47, 120.23, 111.20, 107.65; positive ESI-MS $m/z$ 320 $[M+1]^+$; HR-MS (ESI): Calcd for $C_{13}H_{10}N_3O_5S$ $[M+H]^+$ 320.0341, Found 320.0317.

Compound **4g** (266 mg, 80%): $^1$H-NMR (300 MHz, DMSO-$d_6$) $\delta$: 8.13 (dd, $J$=8.9, 2.3 Hz, 1H), 8.02 (d, $J$=2.3 Hz, 1H), 7.82 (d, $J$=8.2 Hz, 2H), 7.71 (d, $J$=8.9 Hz, 1H), 7.37 (d, $J$=8.2 Hz, 2H), 2.36 (s, 3H); $^{13}$C-NMR (75 MHz, DMSO-$d_6$) $\delta$: 157.18, 148.64, 144.99, 143.33, 139.41, 131.99, 129.89, 126.54, 120.18, 111.16, 107.64, 21.33; positive ESI-MS $m/z$ 334 $[M+1]^+$; HR-MS (ESI): Calcd for $C_{14}H_{12}N_3O_5S$ $[M+H]^+$ 334.0498, Found 334.0477.

**Biological Assays. Cell Culture** Human breast cancer cell lines (MDA-MB-468 and MCF-7) were grown in RPMI-1640 medium with 15% fetal bovine serum (FBS) for 24 h, and then the cells were harvested and counted. Solutions of tested compounds (100 $\mu$L) at the desired concentrations and MCF-7 cell solution ($2.5\times10^4$ cells/mL, 100 $\mu$L) were added incubated. Then, the cell viability was assayed by MTT method.

Each tested compound was dissolved in dimethyl sulfoxide (DMSO) followed by dilution with the medium to desired concentrations, and DMSO final concentration was 0.1% in all of the cultures. DMSO at 0.1% was added control groups and showed no effects on cells. All the cultures were kept in a $CO_2$ incubator under moist condition of 5% $CO_2$ in air at 37°C.

**Cell Viability Assay** Cells were seeded in 96-well plates ($5\times10^4$ cells/well) in triplicate and treated with compounds **3a**–**l**, **4a**–**g** in 1 $\mu$M, 10 $\mu$M, 100 $\mu$M. After a 48 h incubation period, 20 $\mu$L MTT reagent (5 mg/mL) was added, and the cells were incubated for 4 h. The supernatants were aspirated, and the formazan crystals in each well were dissolved in 200 $\mu$L of dimethyl sulfoxide for 30 min at 37°C. The absorbance value was monitored by microplate reader at 490 nm and used to calculate cell viability.

**STAT3 Protein Level Assay** After treatment with **3a**, **3c**, **3d** and **4e** 10 $\mu$M, 100 $\mu$M or DMSO for 24 h, the samples were analyzed for STAT3 using the human signal transducer and activator of transcription 3 (STAT3) Kit (Rapidbio, RB) with an enzyme-linked immunosorbent assay (ELISA)-based method following the manufacturer's protocol. The result was used to calculate the concentration of STAT3 in the samples and the inhibition rate.

**STAT3 Binding Assay with FIA-QCM** Immobilization procedure of STAT3: The immobilization of STAT3 molecules on the surface of quartz crystal microbalance (QCM) chip was carried out as reported method[26] with slight modification. Briefly, the chip surface was first cleaned with Piranha solution ($H_2SO_4$–30% $H_2O_2$=3 : 1, v/v), and rinsed with water and ethanol, then air-dried. The cleaned surfaces were immersed into a 20 mM cysteamine hydrochloride solution for 12 h in the dark at room temperature, and then the excess cysteamine was removed with ethanol and water washings. Glutaric dialdehyde was used as activating reagent to introduce aldehyde groups. The quartz crystal was immersed into a 2.5% (v/v) glutaric dialdehyde solution (pH 7.4) at 40°C for 4 h in an incubator shaker, and stopped by washing with large amount of water. Then, the chip was exposed to 30 $\mu$L of 1.6 $\mu$M STAT3 solution at room temperature for 12 h. In order to eliminate the interference of glutathione contained in the STAT3 solution, a reference chip (QCM-G) was also prepared following the same procedure with only the same concentration of

glutathione solution.

Inhibitors-STAT3 binding assay: At the beginning, 10% DMSO Tris–HCl buffer (50 mM, pH 7.4) was flowed into STAT3 modified chip (QCM-S) *via* the HPLC injection value (flow rate, 40 $\mu$L/min). After a stable baseline was achieved, 200 $\mu$L of **3a** or **3c** solutions (dissolved in 10% DMSO Tris–HCl buffer solution, and the final concentration was 0.5 mg/mL) were injected into the fluid system *via* the HPLC injection value. The curves of frequency *versus* time were recorded and the entire real-time association and dissociation processes were displayed continuously on the computer. The same experiment was conducted on the glutathione modified chip (QCM-G).

**Statistical Analysis** Data are presented as means±S.D. of the indicated number of experiments. Data were analyzed by one-way analysis of variance (ANOVA) followed by Dunnett's test or Student's *t*-test when appropriate. Probability values of 0.05 or less were considered to be statistically significant. All statistic analyses were performed with SPSS 13.0 (SPSS Inc., Chicago, IL, U.S.A.).

**Acknowledgments** This work was supported by the Natural Science Foundation of Jiangsu Province (BK2009240), the National Natural Science Fund for Creative Research Groups of China (21121091) and the fund of Jiangsu Key Laboratory for Molecular and Medical Biotechnology (2011MMBKF02).

**Supplementary Data** Supplementary data (the docking results, $^{1}$H- and $^{13}$C-NMR spectra of selected synthesized compounds) associated with this article can be found, in the online version.

## References

1) Darnell J. E. Jr., *Science*, **277**, 1630–1635 (1997).
2) Horvath C. M., Darnell J. E. Jr., *Curr. Opin. Cell Biol.*, **9**, 233–239 (1997).
3) Zhong Z., Wen Z., Darnell J. E. Jr., *Science*, **264**, 95–98 (1994).
4) Stahl N., Farruggella T. J., Boulton T. G., Zhong Z., Darnell J. E. Jr., Yancopoulos G. D., *Science*, **267**, 1349–1353 (1995).
5) Yu H., Jove R., *Nat. Rev. Cancer*, **4**, 97–105 (2004).
6) Masciocchi D., Gelain A., Villa S., Meneghetti F., Barlocco D., *Future Med. Chem.*, **3**, 567–597 (2011).
7) Timofeeva O. A., Gaponenko V., Lockett S. J., Tarasov S. G., Jiang S., Michejda C. J., Perantoni A. O., Tarasova N. I., *ACS Chem. Biol.*, **2**, 799–809 (2007).
8) Fletcher S., Turkson J., Gunning P. T., *ChemMedChem*, **3**, 1159–1168 (2008).
9) Becker S., Groner B., Müller C. W., *Nature*, **394**, 145–151 (1998).
10) Turkson J., Kim J. S., Zhang S., Yuan J., Huang M., Glenn M., Haura E., Sebti S., Hamilton A. D., Jove R., *Mol. Cancer Ther.*, **3**, 261–269 (2004).
11) Gunning P. T., Katt W. P., Glenn M., Siddiquee K., Kim J. S., Jove R., Sebti S. M., Turkson J., Hamilton A. D., *Bioorg. Med. Chem. Lett.*, **17**, 1875–1878 (2007).
12) Shahani V. M., Yue P. B., Fletcher S., Sharmeen S., Sukhai M. A., Luu D. P., Zhang X. L., Sun H., Zhao W., Schimmer A. D., Turkson J., Gunning P. T., *Bioorg. Med. Chem.*, **19**, 1823–1838 (2011).
13) Siddiquee K. A. Z., Gunning P. T., Glenn M., Katt W. P., Zhang S., Schroeck C., Sebti S. M., Jove R., Hamilton A. D., Turkson J., *ACS Chem. Biol.*, **2**, 787–798 (2007).
14) Bhasin D., Cisek K., Pandharkar T., Regan N., Li C., Pandit B., Lin J., Li P. K., *Bioorg. Med. Chem. Lett.*, **18**, 391–395 (2008).
15) Siddiquee K., Zhang S., Guida W. C., Blaskovich M. A., Greedy B., Lawrence H. R., Yip M. L. R., Jove R., McLaughlin M. M., Lawrence N. J., Sebti S. M., Turkson J., *Proc. Natl. Acad. Sci. U.S.A.*, **104**, 7391–7396 (2007).
16) Matsuno K., Masuda Y., Uehara Y., Sato H., Muroya A., Takahashi O., Yokotagawa T., Furuya T., Okawara T., Otsuka M., Ogo N., Ashizawa T., Oshita C., Tai S., Ishii H., Akiyama Y., Asai A., *ACS Med. Chem. Lett.*, **1**, 371–375 (2010).
17) Zhao M., Jiang B., Gao F. H., *Curr. Med. Chem.*, **18**, 4012–4018 (2011).
18) Irwin J. J., Shoichet B. K., *J. Chem. Inf. Model.*, **45**, 177–182 (2005).
19) Morris G. M., Huey R., Lindstrom W., Sanner M. F., Belew R. K., Goodsell D. S., Olson A. J., *J. Comput. Chem.*, **30**, 2785–2791 (2009).
20) Ichiba T., Yoshida W. Y., Scheuer P. J., Higa T., Gravalos D. G., *J. Am. Chem. Soc.*, **113**, 3173–3174 (1991).
21) Davies J. R., Kane P. D., Moody C. J., *J. Org. Chem.*, **70**, 7305–7316 (2005).
22) Garin J., Melendez E., Merchan F. L., Merino P., Orduna J., Tejero T., *J. Heterocycl. Chem.*, **27**, 321–326 (1990).
23) Meléndez E., Merchán F. L., Merino P., Orduna J., Urchegui R., *J. Heterocycl. Chem.*, **28**, 653–656 (1991).
24) Lai C., Gum R. J., Daly M., Fry E. H., Hutchins C., Abad-Zapatero C., von Geldern T. W., *Bioorg. Med. Chem. Lett.*, **16**, 1807–1810 (2006).
25) Sławiński J., Brzozowski Z., *Eur. J. Med. Chem.*, **41**, 1180–1189 (2006).
26) Lieblein J. C., Ball S., Hutzen B., Sasser A. K., Lin H. J., Huang T. H. M., Hall B. M., Lin J., *BMC Cancer*, **8**, 302–309 (2008).
27) Tuantranont A., Wisitsora-at A., Sritongkham P., Jaruwongrungsee K., *Anal. Chim. Acta*, **687**, 114–128 (2011).
28) Zhang Q., Huang Y., Zhao R., Liu G., Chen Y., *Biosens. Bioelectron.*, **24**, 48–54 (2008).